THE ASTROPHYSICAL JOURNAL, 262:110–119, 1982 November 1

PRECESSING JETS IN SAGITTARIUS A: GAS DYNAMICS IN THE CENTRAL PARSEC OF THE GALAXY

ROBERT L. BROWN
National Radio Astronomy Observatory[1]
Received 1982 January 25; accepted 1982 May 3

ABSTRACT

We suggest that the asymmetric velocity field and the point-reflection symmetry of the radio continuum brightness distribution of the inner parsec of the galaxy can be understood as complementary manifestations of collimated gaseous outflow along twin opposing beams that emanate from a central object. That object appears to be the compact nonthermal radio source Sgr A*. The data are best reproduced by a model in which material is expelled along the rotation axis of Sgr A* and Sgr A* precesses with a period $\sim$2300 yr such that the precession axis is inclined $\sim$49° with respect to the line of sight. On the plane of the sky the jets appear to rotate anticlockwise about an axis having a position angle $\sim$80° (or an inclination of $\sim$41° with respect to the rotation axis of the Galaxy). The western jet lies between the Sun and Sgr A* and appears blueshifted; the eastern jet appears redshifted and is on the far side of Sgr A*. The ejection velocity is $\sim$300 km s^{-1} and the mass loss rate is on the order of 10^{-3} $M_\odot$ yr^{-1}.

The precessing beam description accounts, in a natural way, for specific observations of the gas dynamics that are unexpected from gas in circular rotation. In particular, the enormous line widths, $\Delta v > 100$ km s^{-1}, and localized, multiple-component lines, are subsumed in the gaseous outflow model when the telescope beam encompasses a wide range of spatially and kinematically distinct material. Specific comparisons with the radio continuum and infrared spectroscopic data are made, and tests of this dynamical model are proposed.

Subject headings: galaxies: Milky Way — galaxies: nuclei — particle acceleration — radio sources: general

I. INTRODUCTION

The remarkable maps of 12.8 μm Ne II fine-structure line emission from the galactic center presented by Lacy *et al.* (1979) and Lacy *et al.* (1980) demonstrate that the ionized gas within the central parsec of the galaxy is moving in a highly supersonic, yet ordered, manner. With the high angular resolution afforded by these observations, it is now possible to understand the extremely broad ($\Delta v \sim 500$ km s^{-1}) global Ne II profile noted by Wollman *et al.* (1976, 1977) as a superposition of individual components, clouds, which have central velocities as large as $\pm$260 km s^{-1} and enormous internal velocity dispersions, $\Delta v > 100$ km s^{-1} (FWHM). Most importantly, the velocity field exhibits a high degree of symmetry: a line drawn nearly perpendicular to the galactic equator and just south of the galactic center—as defined by IRS 16 (Becklin *et al.* 1978) or the compact radio source (Brown, Johnston, and Lo 1981)—separates regions of blueshifted Ne II emission from regions that are preferentially redshifted (Lacy *et al.* 1979). This latter observation led Lacy *et al.* (1980) to conclude that the ionized gas was dynamically in circular rotation about the galactic center in a disklike configuration.

[1] National Radio Astronomy Observatory is operated by Associated Universities, Inc., under contract with the National Science Foundation.

The high resolution VLA map of the galactic center (Brown, Johnston, and Lo 1981) shares many important characteristics with the 10 μm map, but, in addition, the low surface brightness emission that can be seen on the radio map, unaffected by extinction, suggests a different interpretation for the dynamics of the ionized gas at the galactic center. Specifically, the radio contours exhibit an S-shaped (point-reflection) symmetry about the galactic center that is one important signature of a precessing twin-nozzle jet such as has been proposed to explain the radio structure of NGC 315 (Bridle *et al.* 1976) and NGC 326 (Ekers *et al.* 1978) and, of course, the galactic object SS 433 (Hjellming and Johnston 1981). Here we interpret the radio structure of the galactic center on the basis of such a twin-jet model; we use the Ne II line emission to constrain the orientation of the jets, and we show that the observations are in good agreement with this dynamical model.

II. SYMMETRIC BEAM MODELS OF SAGITTARIUS A

The high resolution VLA map of the galactic center (Brown, Johnston, and Lo 1981), which we reproduce as Figure 1, shows a surprisingly symmetric radio morphology. Specifically, the contours of low surface brightness thermal bremsstrahlung emission exhibit an S-shaped rotational symmetry about a point nearly

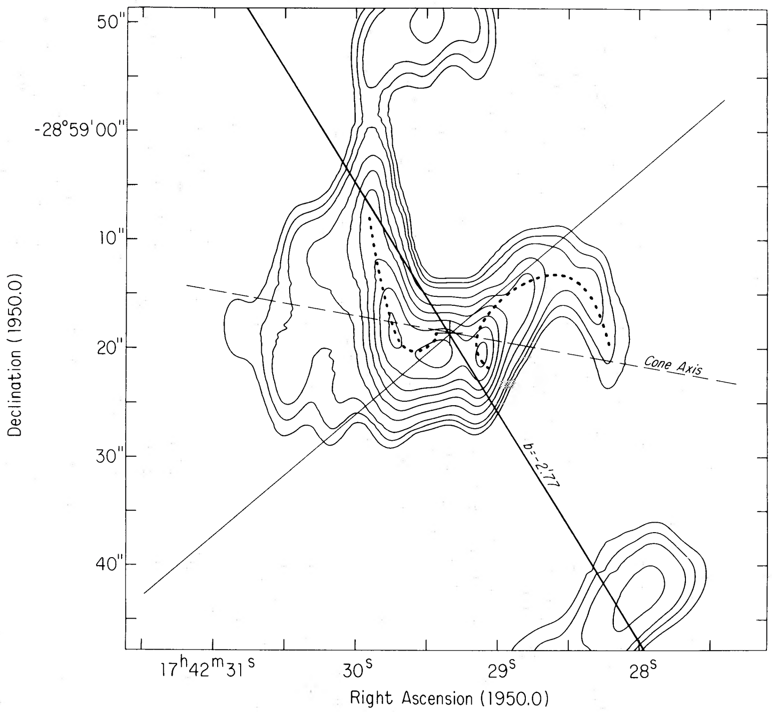

FIG. 1.—The 5 GHz VLA map of the inner parsec of the Galaxy (from Brown, Johnston, and Lo 1981). The position of the compact nonthermal radio source, Sgr A*, is marked by a cross; this source has been removed from the map. The jet precession cone is bounded by the dashed line and the line labeled $b = 2\overset{\prime}{.}77$ that is parallel to the galactic equator. The precession axis is noted. The two dotted lines are drawn in to outline the point-reflection symmetry of the radio structure: these lines are a free representative, not a model fit.

coincident with the bright nonthermal radio core of Sgr A (which we hereafter refer to as Sgr A*). Such curved radio structures are presently quite common in many extragalactic radio sources (see, for example, Heeschen and Wade 1982), and indeed the existence and evolution of such a source morphology is also seen in the galactic star SS 433 (Hjellming and Johnston 1981). The curved symmetry evident in all of these cases is thought to be a manifestation of collimated ejection from opposing jets that emanate from a central object. In this regard the case for SS 433 is particularly compelling owing to the success that such a model has in accounting for the unusual radial velocity behavior of the optical emission lines (Abell and Margon 1979). Furthermore, in addition to a point-reflection symmetry, the twin-jet model will also manifest parallel, structureless contours along a line perpendicular to the jet axis: such features are quite evident on the maps of SS 433 (Hjellming and Johnston 1981) as they are in the map of Sgr A (Fig. 1). Thus, we are led to explore the potential applicability of such a twin-jet interpretation to Sgr A.

Assuming that the central, compact object Sgr A* is the source of twin, opposed, material jets, we may ask how the jets are subsequently curved or bent. Here there seem to be only two real possibilities: (1) ram pressure motion of the external medium, and (2) motion, either rotation or precession, of the nozzle through which the jets emerge. In the former case the ram pressure force of the external medium required to bend the jet through an angle $\Delta\theta$ is $n_0 m_H v_0^2 \sim \dot{p}\Delta\theta/ld$, where $\dot{p}$ is the momentum flux of the bulk motion of the plasma jet, l is the length of the beam over which the force is acting, d is the transverse jet diameter, and n_0 and v_0 are the density and velocity, respectively, of the external medium. Here we may estimate $\dot{p} \approx \rho v_j A_j \approx 1.3 \times 10^{33}$ dyn, where we adopt $\rho \approx 2 \times 10^{-19}$ g cm^{-3} corresponding to the inferred density in the emission clumps (Lacy *et al.* 1980; Brown, Johnston, and Lo 1981), $v_j > 300$ km s^{-1} which is the maximum observed radial velocity and $d \approx 0.1$ pc as representative of the smallest resolved dimensions seen toward Sgr A. Looking at the radio contours to the west of Sgr A* we see $\Delta\theta \sim \pi/2$ over $l \approx 14'' \approx 2 \times 10^{18}$ cm. Since the density n_0 of the external medium exclusive of the dense clumps is $n_0 \leq 40$ cm^{-3} (Watson *et al.* 1980), we find that if the (western) jet is bent by ram pressure of the external medium, then that medium must be flowing (properly rotating, preferentially south to the west of Sgr A* and north to the east of Sgr A*) at a velocity $v_0 \sim c/4$. Because there is no evidence for such a relativistic "wind" at the galactic center, this mechanism appears untenable.

The alternative account of the curved radio contours is that they are a manifestation of a rotation of the nozzles through which the jets emerge. A rotating object will provide the necessary motion if either:

1. The axis of ejection is inclined by $\sim 49°$ with respect to the object's rotation axis, or

2. The axis of ejection is coincident with the rotation axis and the object is precessing.

The former possibility obtains in pulsars where ejection—of highly relativistic particles in an intense magnetic field—occurs along the inclined magnetic axis. The latter is found in SS 433 (Abell and Margon 1979) and in the central object of many extragalactic radio galaxies (Bridle 1982). However, since the collimated material we observe emanating from Sgr A* is thermal gas and the magnetic fields inferred for Sgr A* itself are modest (Reynolds and McKee 1980), Sgr A* appears very similar to SS 433 but markedly different from a pulsar. From this analogy we conclude that precession is the more likely cause of the curved radio contours, and we proceed to their interpretation on this basis. Additionally we note that, as with SS 433, the time for the beams to complete one rotation is so long ($\sim$2000 yr; see below) that the kinetic luminosity of the beam cannot be supplied by an object rotating with this period; hence, we infer that the beam motion reflects precession, not rotation.

The two kinematic features explicit in the Ne II maps of Sgr A of most importance vis-à-vis a precessing twin-beam model are: (1) regions of positive velocity emission are separated from regions of preferentially negative velocity emission by a line drawn perpendicular to the galactic equator that nearly intersects Sgr A*; and (2) regions of the highest Ne II velocity dispersion are found very near Sgr A*. The latter property suggests that mass outflow originates at (or near) Sgr A*, while the former implies that the flow emanates from this point anisotropically. Looking now at the radio map, we can use the lower surface brightness radio contours to allow us to sketch in the cone of precession in a manner similar to that outlined by Hjellming and Johnston (1981); this is shown in Figure 1. We find that such a cone has a large opening angle—49° from the cone axis—and one projected cone edge lies along the line $b = 2\!'\!.77$ that intersects Sgr A*: the projected cone axis in the plane of the sky thus appears inclined $\sim$49° to the galactic equator.

The radio continuum map alone cannot, of course, give us the true orientation of the putative precession cone. However, if a line perpendicular to $b = -2\!'\!.77$ is to divide preferentially positive from negative velocity emission features, then we must be viewing such a twin-jet source nearly along one edge of the precession cone; Figure 2 illustrates the likely orientation. In this case material in the beam on the near side of Sgr A* will appear to the west of Sgr A* at negative velocities; conversely, material in the beam on the far side will appear to the east with positive velocity. We can make this description quantitative: if we note that the position angle of the cone axis (Fig. 1) appears to be $\sim$80° (east from north) and we adopt an ejection velocity of 300 km s^{-1} corresponding to the largest observed Ne II or radio recombination line velocity (Lacy *et al.* 1980; Balick and Wollman 1982), then we can plot the radial velocity field in the vicinity of Sgr A* corresponding to the precession cone and viewing orientation illustrated

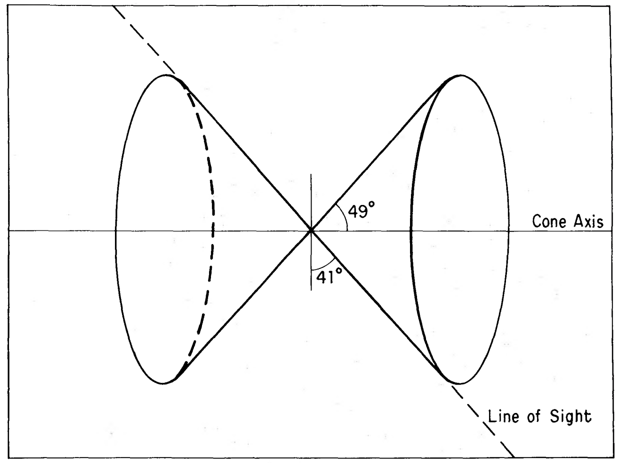

FIG. 2.—The orientation of line of sight (*dashed line*) relative to the axis of the precession cone.

in Figure 2; the resulting plot of permitted radial velocity as a function of position is shown in Figure 3. Here the velocity flow (the intersection in Fig. 3) originates at the position of Sgr A* with material to the west of this position having a preferential blueshift while material to the east appears preferentially redshifted. Exceptions to this pattern, the "peculiar" positive velocities to the west of Sgr A*, or negative velocities to the east, occur when the angle of ejection relative to the line of sight is $>$90° (cf. Fig. 2). Finally, comparing Figures 1 and 3, we see that the sense of precessional rotation is anticlockwise.

At this point let us recapitulate. We have noted that both the symmetric, S-shaped (point-reflection), radio brightness distribution toward Sgr A as well as the asymmetric velocity field in this direction are consistent with, and suggestive of, asymmetric expansion about a point near Sgr A*. The velocity field (but not the radio continuum brightness) is also consistent with rotation about Sgr A* as has been emphasized by Lacy *et al.* (1980). Considering only such general features, it is difficult to discriminate between these two possibilities. However, it is useful to note, once the orientation angles of the twin-jet model have been established, as outlined above, this model makes specific predictions that can be verified. In particular, the profiles of spectral lines at any point in the map can be estimated because the permitted range of velocities, at every point, are determined solely by the radial velocity field (which is known if the ejection velocity is constant). Thus we can compare the twin-jet model, in detail, with the observations.

Let us assume, therefore, that we are indeed dealing with opposing, collimated beams of (principally) thermal material ejected from a central object that is itself precessing in the manner and with the orientation described previously. In this case the radial velocity of spectral lines measured at any point near Sgr A* is obtained by convolving the telescope beam with the field of permitted radial velocities shown in Figure 3. Since

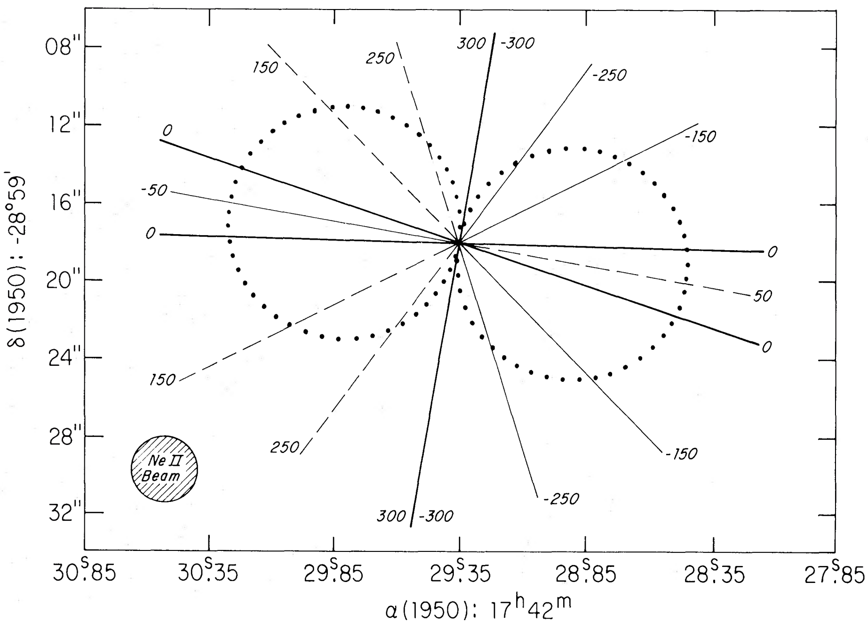

FIG. 3.—The field of permitted radial velocities in the vicinity of Sgr A*, projected in the plane of the sky, corresponding to collimated outflow at $v_e = 300$ km s^{-1} from Sgr A* when viewed with the orientation illustrated in Fig. 2. The dotted lines schematically outline the two precession cones.

the highest resolution spectrographic observations toward Sgr A are the Ne II observations reported by Lacy *et al.* (1980), we have integrated this Ne II telescope beam (FWHM only) over Figure 3 at each point for which Ne II line profiles are available. By doing this, we can compare the permitted range of radial velocity at each point with that actually observed. The results are shown in Figure 4 for four declination strips.

The shaded areas in Figure 4 represent the range of radial velocity permitted in the twin-jet model; the bars illustrate the width (FWHM uncorrected for the 77 km s^{-1} instrumental resolution) of the observed Ne II line profiles reported by Lacy *et al.* (1980). In general the agreement is extremely good—the details are particularly striking.

1. The widest lines are expected, and occur, near Sgr A* where the telescope beam encompasses both the highest positive and negative velocity material.

2. The line width at all positions on the map reflects a convolution, by the telescope beam, of spatially and kinematically discrete material. Thus, we expect to see uncommonly large line widths. (In this model the observed velocity dispersion depends sensitively on telescope beamwidth, and for this reason, the observed velocity dispersion is not representative of internal conditions in any coherent, or distinct, "cloud".)

3. Ne II line profiles that exhibit two identifiable peaks (two velocity components) occur *only* within one beamwidth of the right ascension of Sgr A* [α(1950): 17^{h}42^{m}29^s.35]. Only near this right ascension is it possible for the telescope beam to encompass both sides of one precession half-cone (i.e., the side that is near zero velocity as well as the side at high, positive or negative, velocity) or both precession half-cones.

These detailed comparisons depend on, and are sensitive to, knowledge of the telescope beamwidth and the telescope pointing. If the absolute telescope pointing is only good to $\sim 2''$ while the beam is 3".5 (Lacy *et al.* 1980), then we expect the specific correspondence between theory and observation to be smeared out somewhat. Given this caveat, however, the gross characteristics of the twin-jet model appear sufficiently consistent with the available spectrographic data to warrant a more thorough discussion and application to the galactic center. To this end, we discuss below the time evolution and gas dynamics resulting from collimated outflow that emanates from a precessing object.

III. DISCUSSION AND IMPLICATIONS OF THE COLLIMATED EJECTION MODEL

a) *The Model*

The twin-jet model which we crudely outline above is manifestly a "heavy" jet: once the jet material is expelled from the central source, it must be dominated by, if not composed exclusively of, thermal matter. There is no evidence from the radio continuum observations of Figure 1, or elsewhere, for nonthermal emission in the inner parsec of the galaxy other than that directly associated with the compact source Sgr A*. In this important respect the model we propose for Sgr A* differs from descriptions of its galactic analog SS 433. Motion of the central source—which we presume

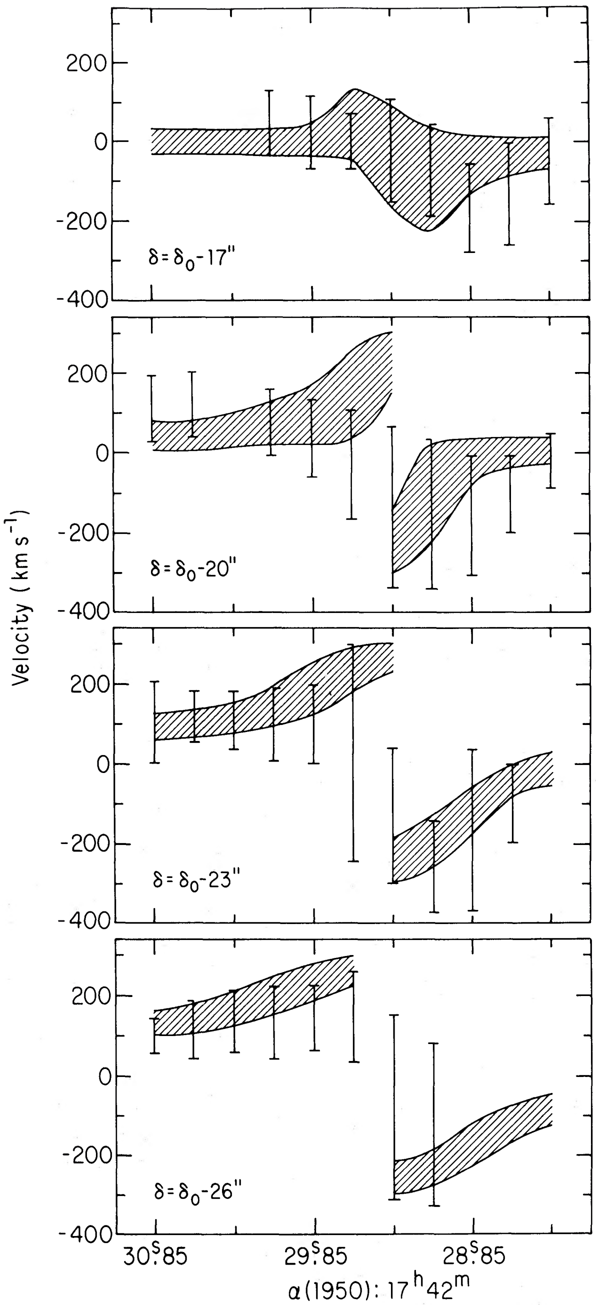

FIG. 4.—The radial velocity as a function of right ascension for four declination strips toward Sgr A*. The shaded areas denote the range of velocities permitted by the velocity field of Fig. 3 when that field is observed with a 3″ circular beam. The bar symbols represent the range of velocity observed (approximate FWHM uncorrected for instrumental resolution) reported by Lacy *et al.* 1980 in the Ne II 12.8 μm fine-structure line.

to be precession—is an integral part of the model that is needed here, as in many extragalactic sources (e.g., Bridle 1982), to provide the symmetric radio morphology.

In order to reconstruct the time evolution of a precessing beam, we need to know both the precessional period and the velocity of expelled material as a function of distance from the central source, Sgr A*. The two are related: consider the latter first. At any time the instantaneous mass of material in the jet is $m_j \approx \frac{1}{2}(dm/dt)\Delta t$ with $\Delta t \approx (\theta_j/2\pi)P$ and where θ_j is the jet opening angle, P is the precession period, and dm/dt is the mass loss rate of Sgr A*. The displacement, x, of this material from the point of ejection as a function of time is

$$m_j \frac{d^2x}{dt^2} = P_0 A_j(x) x^2 \left(\frac{dx}{dt}\right)^2 , \qquad (1)$$

where the term on the right accounts for deceleration by the ambient gas (of mass density ρ_0) and $A_j(x) = \pi x^2 \tan^2(\theta_j/2)$ is the cross sectional area of the jet. Thus the situation is complex: to evaluate equation (1) we must estimate the precession period, the mass loss rate, the jet opening angle, and the ambient density within 1 pc of Sgr A*. We discuss each of these separately.

1. A first approximation to the precession period P can be obtained with the assumption that the jet is undecelerated, $v_j = v_e = 300$ km s^{-1}. Let the rotation angle of the jet about its axis be ψ and define $\psi = 0$ when the two jets appear coincident with the axis of the precession cone such that the western jet is on the far side of its half-cone while the eastern jet is on the near side of its half-cone (cf. Fig. 2). Further, let the angle θ be the angle, on the plane of the sky, between the cone axis and a line joining any point on the map with Sgr A*: thus, for the specific orientation of Figure 2, $\theta = \psi/2$. Looking now at the distant western radio contours of Figure 1 we observe $\theta_1 \approx 19°$ which implies that the jet rotation angle (at ejection) was $\psi_1 \approx 38°$ and that this material was ejected $t_1 \approx 13''.3$ (1.5×10^{12} km arcsec^{-1})/(300 km s^{-1}) ≈ 2100 yr ago. Similarly, the western feature nearest Sgr A* (IRS 2) has $\theta_2 \approx -28°$ so that $\psi_2 = -56° = 304°$ and, as above, $t_2 = 665$ yr. From this we estimate the precession period as $P = \Delta t/\Delta\psi/360° \approx 1950$ yr.

2. The total mass of ionized material as measured by Ne II spectroscopic observations (Lacy *et al.* 1980) or inferred from the radio continuum data (Brown, Johnston, and Lo 1981) ranges from 2–20 $M_\odot$ depending on the extent of clumping present. If, as we are assuming, a significant fraction of this material results from outflow from the central source—and if it accumulates in one precession period, then $dm/dt \approx 2 \times 10^{-3} M_\odot$ yr^{-1}.

3. An estimate of the jet opening angle can be made by identifying this angle with the angle subtended by the smallest scale structure in the radio map as seen from the central position, Sgr A*. At high frequencies, $\nu \geq 15$ GHz, all the small-scale structure present on the

TABLE 1

PARAMETERS OF THE PRECESSING COLLIMATED BEAM MODEL

Parameter	Value
Precession period	2300 yr
Velocity of ejection	300 km s^{-1}
Mass loss rate....................	$2 \times 10^{-3}\ M_{\odot}\ yr^{-1}$
Jet rotation	Anticlockwise about an axis drawn through Sgr A* with a position angle of 80°
Inclination	Jet axis is inclined ~49° with respect to the line of sight (~41° from the axis of galactic rotation)
Jet opening angle	The angle between the jets and the jet rotation axis is 49°

radio continuum map (apart from Sgr A* itself) is confined to the positions of the two bright components nearest Sgr A* (cf. Fig. 1). The scale of this structure, ~2″, at a projected distance of 4″.5, implies a full jet opening angle of $\theta_j \sim 25°$.

4. Watson *et al.* (1980) conclude that the number density of uniformly distributed matter in the inner parsec of the Galaxy is <40 cm^{-3}; we adopt this value for the ambient gas density.

With the parameters noted here, equation (1) can be evaluated and the results, as projected on the sky, can be compared with the radio brightness distribution. Doing this explicitly, we find that a best-fit is obtained with a precession period of 2300 yr, all other parameters retaining their previous values. The properties of the twin-jet model are summarized in Table 1 and discussed below.

b) Comparison with the Observations: General Remarks

The precessing, twin-jet, model is highly predictive. In particular, when the ejection velocity is constant, the position of the beams as a function of time and the velocity (both radial and proper velocity) are well defined at each point on the map. To illustrate this, we plot in Figure 5 the position of the two jets, projected on the plane of the sky, as a function of ejection time for ejection times ranging from 3500 yr ago to 250 yr ago. Points on this figure are noted in steps of 250 yr over this interval, and radial velocities corresponding to a few of these points are indicated in parentheses. In addition, we tabulate in Table 2 many of these same parameters noting for each 250 yr increment ($3500 \leq t \leq 250$ yr) the present observed angular displacement of the beam from Sgr A*, the position angle corresponding to that displacement, the expected radial velocity, and a rough estimate of the gas density in the beam at that point. The density estimate is obtained from

$$n(x) \approx \tfrac{1}{2}(dm/dt)[m_{\rm H}\, A_j(x)(\theta_j/2\pi)P]^{-1}\ . \qquad (2)$$

In principle, comparison with the observations is now straightforward: one convolves the telescope beam with Figure 5. Several factors complicate this procedure however. First, the beam is broadened, both radially, and perpendicular to its direction of propagation by internal turbulence, adiabatic expansion, and by the finite time required for the jet opening angle to sweep past a particular angle θ. For turbulent velocities even as large as $0.1v_e$, this combination of effects will smear the regular pattern of Figure 5 by ~3″ for most θ over times longer

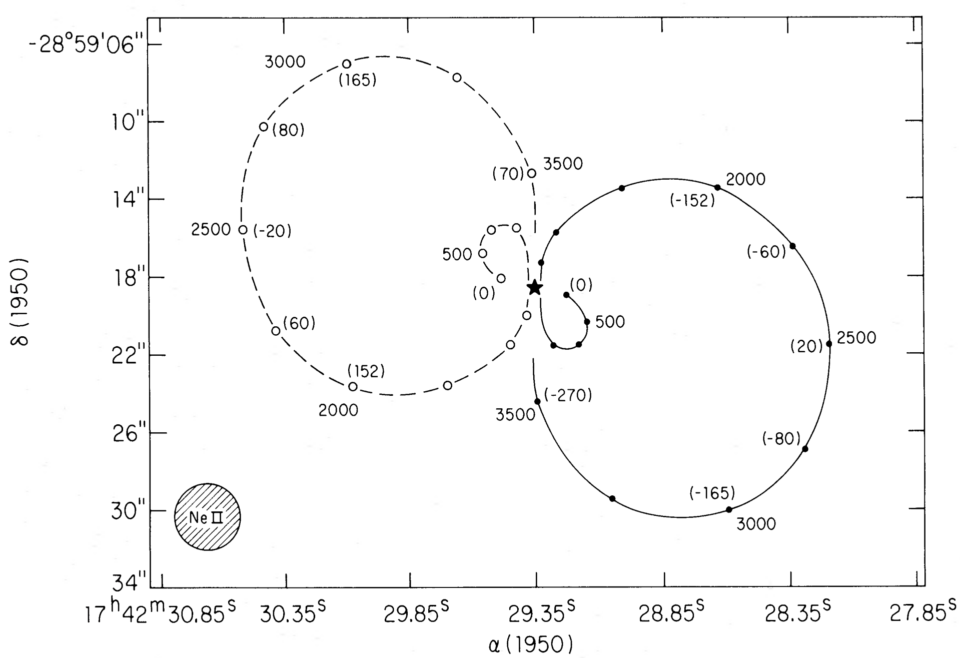

FIG. 5.—The present location of the two precessing beams labeled by the time since ejection. Successive $\Delta t = 250$ yr time increments are noted by a dot on each precession track. The numbers in parentheses are values of the expected radio velocity (km s^{-1}) at the positions noted.

TABLE 2

THE EVOLVING COLLIMATED BEAM MODEL

Time Since Ejection (yr)	Displacement[a] (arcsec)	Position Angle[b] East	Position Angle[b] West	Radial Velocity[c] (km s^{-1})	Density (cm^{-3})
3500	5.8	1	−179	270	2.5×10^3
3250	12	20	−160	230	2.7×10^3
3000	15	40	−140	165	3.2×10^3
2750	16	59	−121	80	3.8×10^3
2500	15	79	−101	−20	4.5×10^3
2250	14	99	−81	60	5.9×10^3
2000	11	118	−62	150	6.8×10^3
1750	6.7	138	−42	230	9.5×10^3
1500	3.2	157	−23	280	1.2×10^4
1250	1.5	165	−15	290	1.8×10^4
1000	3.2	16	−164	260	2.6×10^4
750	3.7	36	−144	190	4.6×10^4
500	3.2	56	−124	100	1.0×10^5
250	1.7	75	−105	0	7.5×10^5
0	...	95	−85	40	...

[a] Maximum apparent angular displacement from the position of Sgr A*.
[b] On the sky, relative to Sgr A*. Angles are measured (positive) east from north.
[c] Tabulated for the eastern jet—multiply by (−1) to obtain values appropriate to the western jet.

than about 1000 yr. Second, the beam position at any time depends critically on the ejection velocity and on the ram pressure deceleration of the beam in the gas surrounding Sgr A*. Here we have assumed a constant ejection velocity, a constant mass ejection rate, and uniformly distributed ambient material; if any of these assumptions is invalid, the observed kinematic effects would be marked.

c) Comparison with the Radio Observations

If one compares the precessing beam map (Fig. 5) with the observations (Fig. 1), good agreement can be seen between our expectations and the observations. Of course, this is not a real surprise because we have relied heavily on the radio map to constrain the model. But, in addition, recent $\lambda 2$ cm VLA observations (R. L. Brown, K. Y. Lo, and K. J. Johnston, unpublished) show that the densest material in the inner parsec of the galaxy is in IRS 2 and 21, the two bright continuum peaks nearest Sgr A* that are evident in Fig. 1. These observations are entirely in accord with our expectations, since we anticipate that these features were both formed within the last 1250 yr, whereas the rest of the map is representative of older material that presently is of lower density (cf. Table 2). The simple precessing beam model also accounts, in a general way, for all the identifiable peaks in the radio map (IRS 2, 4, 5, 6, 10, 21; cf. Brown, Johnston, and Lo 1981) except IRS 1. (In this model the continuum "peaks" indicate nonlinearities or local instabilities in the jet flow, not discrete, long-lived clouds.) In detail, however, the agreement is not entirely satisfactory. The ridge consisting of IRS 1, 5, and 10 is particularly vexing. To account for this spatial feature (and the Ne II velocities which cluster near $+75$ km s^{-1} over the ridge) in the ejection model requires that the eastern beam be slowed considerably from v_e when the apparent position angle of the beam was $\sim 30°$–$60°$. Such an effect would result from either a real change in the ejection velocity or from unusually efficient ram pressure deceleration over this region owing to a local enhancement in the ambient gas density.

It is also clear from a comparison of the model with the observations that if the model is to be viable then the outflow from each of the jets cannot have been constant in time. For example, there seems to be no evidence on the radio map that the western jet was even "on" from roughly 3250 to 2750 yr ago. Nor is there an eastern reflection-symmetric (about Sgr A*) counterpart to the recent ejecta which comprises IRS 2; thus, the eastern jet appears to have been inactive over the past ~ 750 yr.

Twin jet models in which often only one jet is active at a time have been invoked to account for "one-sided" extragalactic radio galaxies (Bridle 1982). Moreover, there is even suggestive evidence that the two opposing jets in twin-jet extragalactic sources alternate, in turn and in phase, periods of activity and inactivity—when one jet is "on," the other is "off" and vice-versa (Rudnick 1982). A similar suggestion also may be present here as well with a duty-cycle of perhaps $P/4$–$P/2$.

Finally, the definitive test of all these ideas is to actually observe the radio jets themselves. This may be possible with VLBI techniques at sufficiently high frequencies (where the effect of interstellar scattering is minimized). If such an observation is feasible, we anticipate Sgr A* presently will appear elongated by its jets along position angle $\sim 95°$ (and/or $-85°$; cf. Table 2).

d) *Spectroscopic Observations*

As we discussed in § II and illustrated in Figure 4, the twin-jet, precessing beam model accounts in a coherent manner for the general kinematic structure within 1 pc of Sgr A* as revealed by the Ne II 12.8 μm spectroscopic observations. Specifically, the separation on the sky between regions of positive velocity from those of negative velocity is directly attributable to our orientation vis-à-vis the axis of the precession cone: to the east we see redshifted outflow from the beam on the far side of Sgr A*, while to the west we see blue-shifted outflow from the jet located between us and Sgr A*. Near the right ascension of Sgr A*, the combination of our viewing orientation and the large Ne II beam causes the two jets to appear superposed and we expect to see very broad lines. All this is in keeping with the sense of the Ne II observations.

In detail, however, the beam model suggests an interpretation of the characteristics of the Ne II observations quite different from that given by Lacy *et al.* (1980), particularly with regard to: (1) the nature of the continuum peaks; (2) the interpretation of the unusually large velocity dispersions; (3) the presence of multiple velocity components along a single line of sight; (4) the ionization and density distribution of thermal material; and (5) gas dynamics in the central parsec of the galaxy.

1. In the beam model thermal continuum peaks are attributable to non-linearities in the outflow from the central source. Such non-linear flow may be amplified by local instabilities that develop downstream, or the flow may *appear* amplified in regions where $d\theta/dt$ is smallest (that is when $\theta \sim 45°$; e.g., the "ridge" prominent to the east of Sgr A*). In either case, the continuum peaks are not coherent structures, they are not gravitationally (or otherwise) bound, and they are not long-lived.

2. The unusually large velocity dispersion noted by Lacy *et al.* (1979; 1980), $\Delta v > 100$ km s^{-1} (4–5 times larger than the value in a typical H II region), is subsumed in the beam model and results from a smearing together, by the telescope beam, of spatially and kinematically distinct parts of the outflow. This can be most easily appreciated in Figures 3 and 4. As a corollary to this, we anticipate that the observed line profiles will be very sensitive to telescope beamwidth—the effect will be greatest where the velocity streamlines are most dense (i.e., near Sgr A*; Fig. 3) and less pronounced away from this position.

3. We expect to observe multiple velocity components when, and only when, the telescope beam encompasses either (*a*) the track of both beams (the east and west) or (*b*) the track of either single beam at two epochs. This occurs only for observations made near the right ascension of Sgr A* as can be seen most clearly in Figure 5. Note, for example, that immediately to the south of Sgr A* the Ne II beam encompasses the eastern beam at $t \approx 1500$ yr as well as the western beam at $t \approx 3500$ yr: since we expect the former to have a radial velocity $+280$ km s^{-1} while the latter has a radial velocity -270 km s^{-1} (Table 2), we expect the observed line to have two such components and an enormous width. Similarly, immediately to the southwest of Sgr A* the telescope beam encompasses both recently ejected material with a radial velocity ~ 0, as well as material ejected 1000–3000 yr ago that has a radial velocity -260 km s^{-1}; again, we can expect two components to the velocity profile of the line. The observations are consistent with these expectations.

4. Since we imagine that much, if not all, the hot thermal material inferred from the radio or infrared continuum maps has been expelled from Sgr A*, the density and ionization structure in the inner parsec will reflect this history. Thus, the density should be greatest near Sgr A* and decrease with distance from this point. On the other hand, the ionization of the 300 km s^{-1} beam material will be frozen-in—it will reflect conditions at the source of ionization (presumable Sgr A*)—and the ionization state will not change significantly with distance from Sgr A*. While not much is known about the ionization structure, other than the inference that the ionizing radiation field must be quite soft (Lacy *et al.* 1980; Watson *et al.* 1981), it appears from high frequency VLA observations that the gas density in the inner parsec of the Galaxy is indeed greatest within 0.2 pc of Sgr A*. Because the most dense material is also the most recently ejected matter, we anticipate that permitted lines that are unquenched at high densities, for example, Brγ, will be most intense near Sgr A* and the observed LSR radial velocity of these lines will be near zero (cf. Table 2). Observations designed to test this prediction must be made with a small, 2″–4″, telescope beam.

5. Lacy *et al.* (1980) interpret the asymmetric velocity field around Sgr A* as evidence for gaseous rotation about a central mass of several times $10^6\ M_\odot$. If instead, the velocity field is representative of asymmetric outflow, not rotation, then no such dynamical estimate of the mass of the central object is germane. Rather, the only estimate of the central mass that can be made is the upper limit obtained by identifying the beam velocity with the escape velocity $v \geq (2GM/R)^{1/2}$: using $v = 300$ km s^{-1} and $R = 3'' = 0.15$ pc (corresponding to the displacement of the brightest structure on the radio map from Sgr A*), we find $M \leq 1.6 \times 10^6\ M_\odot$.

IV. SUMMARIZING DISCUSSION

We suggest that asymmetries in the velocity field in the inner parsec of the Galaxy (as noted in the Ne II spectroscopic observations reported by Lacy *et al.* 1979; 1980) and the point-reflection symmetry apparent in the thermal radio continuum brightness distribution (Brown, Johnston, and Lo 1981) are complementary manifestations of collimated gaseous outflow from opposing beams that emanate from a central object. That object appears to be the compact nonthermal radio source Sgr A*. The data are best reproduced by a model in which the central object precesses with a period ~ 2300 yr such that the precession axis is inclined $\sim 49°$ with respect to the line of sight. The angle between the jets and the jet rotation axis also seems to be $\sim 49°$. On the plane of the sky, the jets appear to rotate anticlockwise about an axis having a position angle of $\sim 80°$. The western jet is blueshifted and lies between the Sun and

Sgr A*, whereas the eastern jet is redshifted and lies on the far side of Sgr A*; the ejection velocity is ~ 300 km s^{-1}.

Although it is difficult to distinguish asymmetric ejection (as outlined here is a very specific form) from rotation, it is worthwhile to note that the precessing beam model accounts, in a natural way, for specific observational features that are unexpected from circular rotation of discrete H II regions. The enormous line widths observed in the inner parsec of the Galaxy are unknown in galactic compact H II regions, but they are an expected manifestation of gaseous outflow where a single telescope beam encompasses a wide range of spatially and kinematically distinct material. Similarly, the specific viewing orientation shown in Figure 2 as projected on the sky (Fig. 5) provides an opportunity for one to see multiple velocity components along a single line of sight when the telescope beam intersects both jets (or a single jet at two epochs): this only occurs near the right ascension of Sgr A*; such multiple-component Ne II spectral lines are indeed seen at the expected locations (Lacy *et al.* 1980). Finally, in an ejection model, the gas density should be greatest near the central source, and this again is in accord with observations.

The precessing beam model has its deficiencies as well. Most obviously, the rate of mass ejection in a single beam cannot have been constant over periods of time comparable with a precession period. This conclusion follows from the clumped appearance of the thermal continuum emission as well as from departures from detailed symmetry and continuity of the low surface brightness radio contours (compare Figs. 1 and 5). For long periods of time, $\Delta t \sim P/4$, it appears as if one jet or the other was simply "off."

If the precessing beam model for Sgr A* is appropriate, then the mass estimates of this central object made by Lacy *et al.* (1980) assuming circular rotation of discrete H II regions are inapplicable. The gas motion is not rotation but directional flow. However, we can learn something about Sgr A* itself. The total radio luminosity of this object is $\sim 10^{34}$ ergs s^{-1} which requires, for its production, a luminosity $\sim 10^{38 \pm 1}$ ergs s^{-1} in relativistic particles according to the models of Reynolds and McKee (1980). If, in addition, we infer that the object is losing mechanical energy at a rate of $\frac{1}{2}(dm/dt)v_e^2 \sim 5.7 \times 10^{37}$ ergs s^{-1} (corresponding to 2×10^{-3} $M_\odot$ yr^{-1} ejected at 300 km s^{-1}) then we have a picture in which the reservoir of relativistic particles (and magnetic fields) is sufficient to provide the radio emission and drive the collimated outflow. The mass loss itself, 2×10^{-3} $M_\odot$ yr^{-1}, must, of course, either be replenished by accretion or derive from a transitory phenomenon in a massive object: speculations along either of these lines are beyond the scope of this paper.

We have one other constraint on the energetics of Sgr A* which comes from the X-ray observations. The ram pressure interaction of the beam material with the ambient gas leads to supersonic shocks which cool from ~ 0.1 keV by the emission of EUV photons and very soft X-rays. The total energy lost via ram pressure deceleration, using the parameters of § II, is 3×10^{36} ergs s^{-1}. This number is not terribly well determined because it is proportional to the mass loss rate and the ambient gas density, neither of which is known precisely. Nevertheless, such a luminosity can be made consistent with the observational results obtained by Watson *et al.* (1982) if the radiation is indeed so soft that it is, in the main, below the energy band of the *Einstein* IPC and HRI detectors (0.5–4.5 keV), and it suffers severe attenuation in traversing the $N_H = 6 \times 10^{22}$ atoms cm^{-2} along the line of sight. Specific calculations along these lines are needed.

Our description of the gas dynamics of the inner parsec of the Galaxy as a result of collimated ejection from a precessing object is particularly attractive because it subsumes several features of the observations—the radio morphology; the enormous velocity dispersion of the Ne II lines; and the existence of multiple velocity components near Sgr A*—that are unaccountable in the circular rotation model. Further, specific predictions can be made: (1) on a milli-arcsecond scale, the radio source Sgr A* should be elongated by its jets along position angle 95° (and/or −85°); (2) the Ne II line profiles should be a sensitive function of telescope beamwidth, particularly near Sgr A* (the smaller the telescope aperture, the narrower the line); (3) the densest gas in the inner parsec of the Galaxy should be very near Sgr A*, and lines from this dense gas should have a LSR radial velocity ~ 0. The last prediction is the most decisive. If the gas near Sgr A* is in large-scale circular rotation as has been suggested by Lacy *et al.* (1980), then unquenched lines such as Brγ from the most dense gas nearest Sgr A* will share that rotation and will exhibit very large velocity dispersions, $\Delta v \sim 300$–500 km s^{-1}. On the other hand, if the precessing beam description is valid, the densest material near Sgr A* is that most recently ejected; unquenched lines such as Brγ from this gas (when observed with small telescope beamwidths) will appear at zero velocity with a velocity dispersion of only $\Delta v \sim 100$ km s^{-1}. Observations designed to investigate all these predictions, together with a thorough theoretical application of the precessing beam model to Sgr A* and its environs, would be most illuminating.

Finally, let us conclude by pointing out a curiosity for which we have no explanation but which is potentially of great interest. That is, although both the radio brightness and the 10 μm infrared maps of the inner parsec of the Galaxy are strikingly symmetric, the center of symmetry is clearly displaced by $\sim 3''$ from the compact nonthermal radio source Sgr A*. Throughout this work we have assumed that Sgr A* is the source of mass ejection and, by implication, the dynamical center of the Galaxy. But, given the displacement of Sgr A* from the center of symmetry, one might well ask: Does Sgr A* define the dynamical center of the Galaxy or is it rather a companion to a massive, dark, central object?

I am grateful to Drs. M. Rees, R. Sancisi, E. Wollman, and R. Ekers for helpful discussions.

REFERENCES

Abell, G. O., and Margon, B. 1979, *Nature*, **279**, 701.
Balick, B., and Wollman, E. R. 1982, *Proc. JPL Conference on the Galactic Center*, ed. G. Riegler and K. Y. Lo, in press.
Bridle, A. H. 1982, in *IAU Symposium 97, Extragalactic Radio Sources*, ed. D. S. Heeschen and C. M. Wade (Dordrecht: Reidel), p. 121.
Bridle, A. H., Davis, M. M., Meloy, D. A., Fomalont, E. B., Strom, R. G., and Willis, A. G. 1976, *Nature*, **262**, 179.
Brown, R. L., Johnston, K. J., and Lo, K. Y. 1981, *Ap. J.*, **250**, 155.
Ekers, R. D., Fanti, R., Lari, C., and Parma, P. 1978, *Nature*, **276**, 588.
Heeschen, D. S., and Wade, C. M. 1982, in *IAU Symposium 97, Extragalactic Radio Sources* (Dordrecht: Reidel), in press.
Hjellming, R. M., and Johnston, K. J. 1981, *Ap. J.* (*Letters*), **246**, L141.
Lacy, J. H., Baas, F., Townes, C. H., and Geballe, T. R. 1979, *Ap. J.* (*Letters*), **227**, L17.
Lacy, J. H., Townes, C. H., Geballe, T. R., and Hollenbach, D. J. 1980, *Ap. J.*, **241**, 132.
Reynolds, S. P., and McKee, C. F. 1980, *Ap. J.*, **239**, 893.
Rudnick, L. 1982, in *IAU Symposium 97, Extragalactic Radio Sources*, ed. D. S. Heeschen and C. M. Wade (Dordrecht: Reidel), p. 47.
Watson, D. M., Storey, J. W. V., Townes, C. H., and Haller, E. E. 1980, *Ap. J.* (*Letters*), **241**, L43.
Watson, M. G., Willingale, R., Grindlay, J. E., and Hertz, P. 1981, *Ap. J.*, **250**, 142.
Wollman, G. R., Geballe, T. R., Lacy, J. H., Townes, C. H., and Rank, D. M. 1976, *Ap. J.* (*Letters*), **205**, L5.
———. 1977, *Ap. J.* (*Letters*), **218**, L103.

ROBERT L. BROWN: National Radio Astronomy Observatory, Edgemont Road, Charlottesville, VA 22901